Photobiomodulation of immune crosstalk rescues neuroinflammation in Alzheimer's disease models

Qi Shen,[1,2,†] Haocai Chang,[1,2,†] Junyu Li,[1,2,†] Haoyun Guo,[1,2] Wenbin Shi,[1,2] Yihua Yan,[1,2] Wenwen Ouyang,[1,2] Zhan Zhang,[3,4] Xiaolei Wu,[5] Da Xing[1,2] and Sihua Yang[1,2]

[†]**These authors contributed equally to this work.**

Abstract

Peripheral immune cell infiltration and crosstalk with brain-resident cells critically drive Alzheimer's disease (AD)-associated neuroinflammation, highlighting its therapeutic potential.

Here, we found that photobiomodulation (PBM) markedly reduced cerebral $CD8^+$ T cells infiltration in the cortex of AD (APP/PS1 and 3×Tg) mice, thereby improving cognition, and alleviating AD-related pathology by mitigating neuronal damage and gliosis. Immunofluorescence and transcriptomic analyses revealed that PBM inhibited the release of chemokines and pro-inflammatory cytokines from microglia, reducing endothelial adhesion molecules-mediated T cell migration. Concurrently, reduced secretion of tumor necrosis factor-α, interleukin-1α, and complement component 1q by pro-inflammatory microglia further diminished neurotoxic A1 astrocyte induction. Genetic overexpression or pharmacological inhibition further validated that PBM disrupted microglia NOD-like receptor protein 3 inflammasomes activation, attenuating astrocyte reactivity and T cells recruitment.

These findings collectively suggest that the PBM-induced modulation of crosstalk between microglia, astrocytes, and $CD8^+$ T cells is closely related to cognitive improvement. Reprogramming central-peripheral immune crosstalk with PBM resolves neuroinflammation and restores cognition in AD models-a translatable strategy for combating neurodegeneration.

Author affiliations:

1 MOE Key Laboratory of Laser Life Science & Institute of Laser Life Science, College of Biophotonics, School of Optoelectronic Science and Engineering, South China Normal University, Guangzhou 510631, China

2 Guangdong Provincial Key Laboratory of Laser Life Science, College of Biophotonics, School of Optoelectronic Science and Engineering, South China Normal University, Guangzhou 510631, China

3 Department of Neurology, Sun Yat-sen Memorial Hospital, Sun Yat-sen University, Guangzhou 510120, China

4 Guangdong Province Key Laboratory of Brain Function and Disease, Zhongshan School of Medicine, Sun Yat-sen University, Guangzhou 510120, China

5 Department of Neurology and State Key Laboratory of Biotherapy, West China Hospital, Sichuan University, Chengdu 610041, China

Correspondence to: Sihua Yang

MOE Key laboratory of Laser Life Science & Institute of Laser Life Science

College of Biophotonics, School of Optoelectronic Science and Engineering

South China Normal University

No. 55, West Zhongshan Avenue, Tianhe District, Guangzhou

Guangdong Province 510631, China

E-mail: yangsh@scnu.edu.cn

Correspondence may also be addressed to Da Xing

E-mail: xingda@scnu.edu.cn

Running title: PBM and immune crosstalk in AD

Keywords: Alzheimer's disease; neuroinflammation; photobiomodulation; central-peripheral immune crosstalk; $CD8^+$ T cells

Introduction

Alzheimer's disease (AD) is an age and sex related progressive neurodegenerative disease, characterized by cognitive decline and presenting hallmarks including amyloid-β (Aβ) deposition, neurofibrillary tangles, and prominent neuroinflammation[1,2]. These pathological features lead to neuronal cell death, synaptic degradation, and gliosis, involving both microglia and astrocytes, thereby exacerbating neurodegeneration processes[3]. Recent studies have highlighted alterations in brain-resident and peripheral immune cells as well as crosstalk between innate and adaptive immune cells in the development of AD pathology[4-8]. In physiological conditions, microglia serve predominantly protective roles, including the phagocytosis and degradation of Aβ, secretion of anti-inflammatory cytokines, and remodeling of neural networks. However, persistent Aβ accumulation triggers NOD-like receptor protein 3 (NLRP3) inflammasome activation, polarizing microglia toward a pro-inflammatory (M1) phenotype that releases tumor necrosis factor-α (TNF-α), interleukin-1α (IL-1α), and complement component 1q (C1q), collectively termed TIC[9,10]. This pathological cycle compromises the integrity of the blood-brain barrier (BBB) and lymphatic drainage, facilitating the infiltration of immune cell, particularly T cells, into the brain parenchyma and border zone. This, in turn, triggers immune cell activation, antigen accumulation, and T cell receptor clonal expansion[11]. The latest research findings highlight that the infiltration of $CD8^+$ T cells into the brain drives axon degeneration in normally aging mice[12], and their interactions with brain resident cells contribute to AD pathology[13]. But Su et al.[14] identified a type of brain resident $CD8^+$ T cells that coexpress CXCR6 and PD-1. This $CD8^+$ T cells rely on CXCL16-CXCR6 receptor ligand interactions and interact with microglia, thereby limiting the development of AD. Adaptive immune cells show both deleterious and protective effects in AD pathogenesis[15-17], possibly attributed to temporal regulation or functional heterogeneity of the adaptive immune system. Despite advances in understanding central-peripheral immune crosstalk, strategies to modulate this interplay remain underexplored.

The discovery of meningeal lymphatic vessels (mLVs) in the dura has unveiled an extensive lymphatic drainage network within central nervous system (CNS), playing pivotal roles in waste clearance, immune cell trafficking, and maintaining immune homeostasis[18,19]. Transcriptome analysis of mouse meningeal lymphatic endothelial cells

(LECs), microglia, and cerebral blood endothelial cells (BECs) revealed that the meningeal lymphatic function in AD patients is associated with the microglia and brain vascular activation[20], supporting the potential role in modulating the neuroinflammatory responses. The existence of mLVs highlights a crucial link between the central and peripheral immune system, affecting inflammation reaction. Based on extensive research in recent years, crosstalk between the central and the peripheral immune system occurs via these three possible routes[21-24]: BBB, choroid plexus, and meninges. Notably, BBB impairment, an aging risk factor, has been linked to the presence of peripheral immune cells, particularly T cells, in the brains of the elderly and patients with age-associated neurodegenerative diseases[25-27]. Studies in humans and AD animal models have shown that infiltration and clonal expansion of cytotoxic $CD8^+$ T cells in the brains/CSF correlates with a disease progression, suggesting their roles in AD pathogenesis[28,29]. However, direct causative evidence is lacking. Interventions such as vascular endothelial growth factor C (VEGF-C) overexpression[20] or multisensory 40 Hz stimulation[30] improve glymphatic clearance and reduce Aβ burden, but their mechanistic ties to microglial NLRP3 signaling remain unclear.

Non-invasive photobiomodulation (PBM) has shown promise in modulating neuroimmune interactions. Transcranial photobiomodulation reduces Aβ burden and enhances cognitive function in AD models[31], potentially by improving meningeal lymphatic drainage[32]. However, whether PBM directly targets NLRP3-driven neuroinflammation or regulates $CD8^+$ T cell infiltration via endothelial adhesion molecules remains unresolved. And the mechanism of association between the biological effects produced by this modulation in AD remains unknown, and communication systems among brain resident cells and peripheral immune cells in PBM-treated AD models are unresolved.

In this study, we provide evidence that non-invasive PBM mitigates AD-associated neuroinflammation by suppressing NLRP3 inflammasome activation in microglia, thereby disrupting chemokine-mediated $CD8^+$ T cell recruitment and neurotoxic astrocyte induction. Using APP/PS1 and 3×Tg AD models, we demonstrate that PBM therapy enhances lymphatic drainage, reduces Aβ-dependent NLRP3 activation, and inhibits endothelial VCAM1/ICAM1 upregulation-a prerequisite for T cell transendothelial migration. Our findings establish photobiomodulation as a multimodal regulator of central-peripheral immune crosstalk, offering a translatable strategy to break the neuroinflammatory loop in AD.

Materials and methods

Detailed methods are provided in the Supplementary Material.

Animals

C57BL/6, APP/PS1, and 3×Tg mice on a C57BL/6 background were obtained from Guangdong Medical Laboratory Animal Center and Jackson Laboratory. Male APP/PS1 and 3×Tg mice aged 6 months were used. All procedures were approved by the Institutional Animal Care and Use Committee of South China Normal University, Guangzhou, China. Mice were housed under standard conditions with ad libitum access to food and water.

Photobiomodulation treatments

PBM was performed as previously described using a 635 nm semiconductor laser[33,34]. Mice were irradiated on depilated heads for 10 min/day for 4 weeks, delivering 2 J/cm^2 at the hippocampus (~30% transmittance) without detectable thermal effects. Control groups were handled identically without irradiation. BV2 cells and primary neurons were treated with the same parameters for 5 min.

Statistical analysis

Experimenters were blind to the group allocation of mice in all the experiments during data collection and analysis. Data are presented as the means ± standard error of mean (means ± SEM). Statistical analysis was performed with GraphPad Prism 10.0 software, including unpaired t-tests, one- or two-way ANOVA with appropriate post hoc tests, and Spearman correlation. Significance was set at $p < 0.05$.

Results

Photobiomodulation rescues cognitive deficits and attenuates Aβ-driven neuroinflammatory cascades in AD models

To systematically evaluate the therapeutic potential of transcranial PBM therapy, we first assessed its effects on cognitive function and amyloid pathology in APP/PS1 and 3×Tg AD mice. Four weeks of daily 635 nm PBM treatment (10 min/session) significantly improved performance in three behavioral paradigms (Fig. 1A-D). In the novel object recognition (NOR) test, PBM-treated AD mice exhibited a 1.3-fold increase in novel object exploration time compared to untreated controls (Fig. 1B, Supplementary Fig. 1A and B), indicating restored episodic memory. Spatial working memory, as measured by spontaneous alternation in the Y-maze, increased by 40% in PBM-treated APP/PS1 mice and increased by 56% in PBM-treated 3×Tg mice (Fig. 1C), with no

changes in locomotor activity (Supplementary Fig. 1C and D), ruling out confounding motor effects. Fear conditioning assays further revealed a nearly 5-fold in freezing time (Fig. 1D), demonstrating enhanced contextual fear memory consolidation.

To further explore the molecular mechanism by which photobiomodulation improves AD cognition, we carried out a transcriptome analysis by RNA sequencing (RNA-seq). Compared to WT mice, Gene Ontology (GO) functional enrichment analysis of AD mice revealed significant alterations in the expression of genes associated with immune and inflammatory responses (Supplementary Fig. 2). Volcano plot showed expression levels of different genes between AD mice treated with or without PBM (Fig. 1E and Supplementary Fig. 3A). RNA-seq analysis identified 604 differentially expressed genes (DESeq, P value < 0.05) in PBM-treated 3×Tg mice, with downregulation of *Trem2* (-1.9-fold), *Casp1* (-1.3-fold), and *C1qa* (-1.2-fold) - key regulators of microglial activation and inflammasome signaling (Fig. 1E). GO functional enrichment analysis showed changes in gene sets involved in synaptic plasticity, inflammatory response, chemotaxis, neurogenesis and development (Fig. 1F and Supplementary Fig. 3B). Kyoto Encyclopedia of Genes and Genomes (KEGG) terms enrichment also revealed transcriptional alterations related to chemokine signaling pathway, calcium signaling pathway, glutamatergic synapse, long-term potentiation, and NF-κB signaling pathway, which participate in synaptic transmission and neuroinflammation (Fig. 1G and Supplementary Fig. 3C).

NLRP3, apoptosis-associated speck-like protein (ASC), and pro-caspase-1 forms the NLRP3 inflammasome that initiates the production of the proinflammatory cytokine, such as IL-1β and IL-18[35]. As shown in Figure 1H-J, ASC was found to colocalize with Aβ in the brains of AD mice using immunofluorescence staining. However, exposure to PBM resulted in a remarkable reduction in Aβ and ASC in the cerebral cortex and hippocampus DG region, as well as a decrease in the volume of colocalized Aβ and ASC specks in the APP/PS1 and 3×Tg mice, while almost no ASC and Aβ labeling were detected in WT mice (Fig. 1H, I and Supplementary Fig. 4A and B). To determine if there was a relationship between the performance of behavior test and Aβ load, we performed correlation analysis. The levels of Aβ were negatively correlated with novel recognition index (Supplementary Fig. 5E and F). Additionally, the onset of AD often leads to synaptic damage, which can be caused by inflammation activation or impaired function of glial cells[36]. Additionally, because cognitive impairment in AD is closely associated with synaptic structural loss, we used Golgi-Cox staining to evaluate dendritic spine density as a morphological

correlate of synaptic integrity in the cortex of AD mice. Compared to WT littermates, APP/PS1 and 3×Tg mice exhibited a significant reduction in dendritic spine density. Notably, PBM treatment effectively restored dendritic spine density in APP/PS1 mice to levels comparable to those of WT, demonstrating a reversal of synapse loss (Supplementary Fig. 4C and D). To further determine whether PBM affects not only deposited amyloid burden but also soluble Aβ species, we analyzed the soluble cortical fraction from APP/PS1 and 3×Tg mice. Dot blot analysis with the oligomer-preferring antibody A11 revealed a reduction in soluble oligomeric Aβ after PBM treatment in both AD models (Supplementary Fig. 4K). In parallel, 6E10 dot blot analysis showed a concomitant decrease in the overall soluble Aβ-related signal. Synthetic Aβ42 oligomers and Aβ42 monomer peptide were included as reference controls, supporting the interpretation of the oligomeric Aβ readout. Consistent with these dot blot results, ELISA further demonstrated that PBM reduced soluble $A\beta_{1\text{-}40}$ and $A\beta_{1\text{-}42}$ levels in the cortex of both APP/PS1 and 3×Tg mice (Supplementary Fig. 4L). These findings suggest that the effect of PBM is not limited to amyloid plaque burden, but may also extend to the soluble Aβ pool, including oligomeric species considered particularly relevant to AD-associated neurotoxicity. In parallel, neuroinflammation in the hippocampus and cerebral cortex of AD mice was evaluated by quantitative analysis of proinflammatory cytokines and immunostaining for GFAP (glial fibrillary acidic protein, an astrocyte marker) and Iba1 (Ionized calcium-binding adapter protein 1, a microglial marker). The results demonstrated that PBM clearly inhibited the AD-induced upregulation of pro-inflammatory gene expression (Fig. 1K and Supplementary Fig. 4E-J) and suppressed the activation of microglia and astrocytes (Supplementary Fig. 5A-D). Moreover, the $Iba1^+$ area and $GFAP^+$ area showed a positively correlation with Aβ load in the cortex and hippocampus of mice, respectively (Supplementary Fig. 5G, H and Supplementary Fig. 5I, J).

Together, these results indicated that PBM treatment might contribute to regulation of neuroinflammation for AD amelioration.

Inhibiting $CD8^+$ T cell infiltration by PBM rescues neuronal damage

Even under homeostatic conditions, microglia maintain contact with peripheral immune cells and astrocytes, allowing them to constantly monitor the condition of the brain[37]. Immunofluorescence analysis revealed a pronounced reduction in parenchymal $CD8^+$ T cell infiltration following photobiomodulation, with a 59% decrease in APP/PS1 mice and a 75% decrease in 3×Tg mice compared with untreated controls (Fig. 2A and Supplementary Fig. 6A). This reduction in $CD8^+$

T cell accumulation was accompanied by a marked decrease in TUNEL (terminal deoxynucleotidyl transferase dUTP nick end labeling)-positive (apoptotic) cell death in the cortex of AD mice (Fig. 2A and D), indicating alleviation of cytotoxic neuronal damage. Additionally, a negative correlation was observed between the number of $CD8^+$ T cells and the novel recognition index in the NOR test (Supplementary Fig. 6B), indicating that the accumulation of $CD8^+$ T cells in the brain is closely associated with cognitive impairments. A hallmark of neurodegeneration-associated $CD8^+$ T cells was the enrichment of granzyme A and perforin, both of which are cytotoxic proteins[29,38,39]. These infiltrating lymphocytes exhibited diminished expression of cytotoxic effectors granzyme A and perforin, suggesting PBM therapy disrupts their neurotoxic potential (Fig. 2B-F).

The pathogenic role of $CD8^+$ T cells was further corroborated *in vitro*, where activated $CD8^+$ T cells directly induced damage in primary cortical neurons (Fig. 2G). Interestingly, while PBM protected neurons from dendritic damage caused by Aβ, this neuroprotective effect was diminished in the presence of cytotoxic $CD8^+$ T cells or in co-culture with their conditioned medium (Fig. 2G and H), underscoring their dominant role in neuronal damage. Importantly, $CD8^+$ T cell depletion via CD8α-neutralizing antibodies replicated the neuroprotective effects of PBM treatment, resulting in a 1.77-fold increase in $NeuN^+$ neuronal density and a 1.04-fold increase in PSD-95 expression in APP/PS1 mice, as well as a 2.79-fold and 1.79-fold increase, respectively, in 3×Tg mice (Fig. 2I-K and Supplementary Fig. 7A), further validating their pathogenic contribution. And A1-like astrocytes activation exhibited a reduction following CD8α neutralizing antibody treatment (Supplementary Fig. 7B and C). Altogether, these findings demonstrate that PBM-mediated suppression of $CD8^+$ T cell infiltration and cytotoxic activity constitutes a key mechanism by which central-peripheral immune crosstalk is rebalanced, thereby alleviating neuronal injury and preserving synaptic integrity in Alzheimer's disease.

PBM treatment suppresses microglia-driven chemokine signaling to limit $CD8^+$ T cell recruitment

The migration of leukocytes across the BBB is a complex process, which is initiated by inflammatory and chemotactic signals released from the CNS[40]. To dissect how PBM modulates $CD8^+$ T cell trafficking, we first interrogated chemokine networks linking microglial activation to endothelial adhesion. In APP/PS1 mice, BECs exhibited a 4.5-fold increase in VCAM1 and 4.8-fold increase in ICAM1 expression compared to WT ($P < 0.0001$;

Fig. 3A-D), consistent with heightened leukocyte adhesion[41,42]. PBM treatment reduced VCAM1 and ICAM1 levels by 66% and 65%, respectively ($P < 0.001$), mirroring the attenuation of $CD8^+$ T cell infiltration observed *in vivo* (Fig. 2A-C). And in 3×Tg mice, BECs exhibited a 3.9-fold increase in VCAM1 and 4.2-fold increase in ICAM1 expression compared to WT, PBM treatment reduced VCAM1 and ICAM1 levels by 79% and 71%, respectively ($P < 0.0001$; Fig. 3A-D). RNA-seq analysis of PBM-treated AD mice further revealed consistent downregulation of pro-inflammatory genes (e.g., *Cd68, Trem2, Casp1, C1qa*) and chemotaxis-associated genes (e.g., *Ccl3, Cxcr2, Cxcl1*). These results suggest that pro-inflammatory microglia release chemokines and pro-inflammatory cytokines, exacerbating the transendothelial migration of $CD8^+$ T cells, neuroinflammation and neuronal dysfunction. PBM treatment mitigates these pathological processes by suppressing chemokine-driven $CD8^+$ T cell recruitment, remodeling the brain microenvironment, and potentially alleviating AD-associated cognitive deficits.

Recent studies have highlighted a tight association between $CD8^+$ T cells, microglia, and neuronal structures in the brain parenchyma of APP/PS1 transgenic mice[43]. Pro-inflammatory microglia secrete TNF-α, which activates BECs and induces the upregulation of adhesion molecules such as VCAM1 and ICAM1, thereby enhancing T cells migration across the BBB[44]. To evaluate whether PBM treatment could inhibit this process, we measured TIC levels in serum and brain tissue using ELISA and assessed transcription levels via RT-PCR (Fig. 3F-L). ELISA and RT-PCR results showed significantly elevated TIC levels in AD mice compared to WT controls, which were markedly reduced following PBM treatment (Fig. 3F-L). Further analysis of individual chemokine ligand-receptor pairs revealed that CXCL16-CXCR6, CCL3-CCR5, CCL4-CCR5, CCL2-CCR2/CCR5/CXCR3, CCL8-CCR2/CCR5 were ligand receptor pairs between microglia and $CD8^+$ T cells[14,42]. Therefore, we further analyzed the expression of TNF-α and the aforementioned chemotactic factors in microglia using flow cytometry. There was a reduction of TNF-α (24%, $P < 0.05$), CCL3 (15%, $P < 0.05$), and CCL4 (36%, $P < 0.001$) in microglia from PBM-treated APP/PS1 mice respectively, compared to untreated APP/PS1 mice (Supplementary Fig. 8A and B). While in 3×Tg mice, TNF-α (25%, $P < 0.05$), CCL4 (18%, $P < 0.01$) and CCL8 (26%, $P < 0.05$) expression were significantly decreased (Supplementary Fig. 8A and B). Notably, microglial TNF-α levels positively correlated with VCAM1 expression ($r = 0.77$, $P < 0.001$; Supplementary Fig. 8D), ICAM1 expression ($r = 0.69$, $P < 0.01$; Supplementary Fig. 8E) and $CD8^+$ T cell abundance ($r = 0.55$, $P < 0.05$; Supplementary Fig. 8F), supporting a causal chain wherein PBM silences microglial inflammatory signals to normalize vascular adhesion molecule expression. These findings suggest that PBM treatment alleviates nerve injury by inhibiting the secretion of TNF-α and chemokines from microglia, thereby reducing

the migration of $CD8^+$ T cells. This mechanism highlights the therapeutic potential of photobiomodulation in mitigating neuroinflammation and neuronal damage in AD.

PBM treatment suppresses pro-inflammatory microglial polarization associated with NLRP3 signaling

In AD, persistent Aβ accumulation strongly activates pro-inflammatory microglia, commonly referred to as M1 microglia[45]. Over time, acute and favorable microglia-mediated inflammation becomes chronic and detrimental[46]. To assess whether photobiomodulation alters microglial activation, we performed immunofluorescence co-staining for Iba1 (pan-microglial marker) and inducible nitric oxide synthase (iNOS, pro-inflammatory microglia polarization marker) in cortical and hippocampal regions. Ramified microglia represent a homeostatic state, whereas ramified morphology indicates activation[47]. The proportion of $iNOS^+$ microglia increased in the cortex of AD mice compared with WT controls (16.9-fold increase in APP/PS1, $P < 0.0001$; 13.9-fold increase in 3×Tg, $P < 0.001$) (Fig. 4A-F). PBM treatment profoundly reduced this population by 88% in APP/PS1 mice ($P < 0.0001$) and 82% in 3×Tg mice ($P < 0.01$), concomitant with a shift toward a ramified, homeostatic morphology (Fig. 4A-F). In the hippocampal region, $iNOS^+$ expression was also found to increase in AD mice compared with WT controls (14.3-fold increase in APP/PS1, $P < 0.0001$; 10.7-fold increase in 3×Tg, $P < 0.01$), and decreased by 78% ($P < 0.001$) and 86% ($P < 0.01$), respectively, after PBM treatment (Fig. 4A-F). Morphometric analysis showed that the diameter of microglial cell bodies in the cortex and the hippocampus of PBM-treated APP/PS1 mice were reduced by 38% ($P < 0.0001$) and 42% ($P < 0.0001$), both of which were close to the level of the corresponding region of WT (Fig. 4G and H). Also in 3×Tg mice, PBM-treated microglial body diameters in the cortex and hippocampus were reduced by 28% ($P < 0.0001$) and 22% ($P < 0.05$), respectively (Fig. 4G and H). Critically, in cortex, microglial soma size correlated strongly with both Aβ plaque burden ($r = 0.80$, $P < 0.0001$; Fig. 4I) and parenchymal $CD8^+$ T cell density ($r = 0.83$, $P < 0.0001$; Fig. 4Q), positioning pro-inflammatory microglia at the intersection of amyloid pathology and neuroimmune dysregulation.

Consistent with these morphological and phenotypic changes, PBM treatment was associated with marked suppression of NLRP3 inflammasome signaling. Western blot and RT-PCR analyses revealed reductions in NLRP3 protein levels by 30% in APP/PS1 mice ($P < 0.05$) and 44% in 3×Tg mice ($P < 0.001$; Fig. 4J and M), accompanied by a 53% and 59% decrease in ASC expression, respectively ($P < 0.05$; Fig. 4J and N). Consistently, transcriptome analysis revealed that PBM treatment led to the downregulation of pro-inflammatory and chemotaxis-associated genes, including *Ccl3*, *Cd68*, *Casp1*, *Icam1*, *Cx3cl1*, and *Trem2* (Fig. 3E). Meanwhile, iNOS protein expression decreased by 48% and

46%, respectively ($P < 0.01$; Fig. 4J and K), confirming broad inhibition of pro-inflammatory pathways. The results of flow cytometry experiments also indicated that the AD model leads to the activation of pro-inflammatory microglia, while PBM treatment inhibits this effect, but does not change the number of M1 microglia (Supplementary Fig. 9).

Importantly, the attenuation of pro-inflammatory microglial polarization coincided with reduced secretion of TNF-α and chemokines (Fig. 3F, M), factors previously linked to endothelial activation and T cell recruitment[41,42]. Together, these data indicate that photobiomodulation shifts microglia away from neurotoxic inflammatory states, thereby reshaping the local immune milieu in a manner permissive to reduced $CD8^+$ T cell infiltration and downstream neuroinflammatory damages.

PBM treatment mitigates microglia-associated A1-like astrocytes activation in AD

To further investigate the influence of TIC alterations on the balance between neurotoxic astrocytes and neurotrophic astrocytes[48], we assessed astrocytes activation and its correlation with cell size. Initially, we measured the size of activated astrocyte ($GFAP^+$) in the cortex and hippocampus of each group (Fig. 5A). Our results showed that astrocytes in the WT group exhibited smaller cell sizes compared to those in the AD group. Notably, PBM treatment significantly reduced astrocyte size in APP/PS1 mice by 62% ($P < 0.0001$), and in 3×Tg mice by 62% ($P < 0.0001$), respectively (Fig. 5B), with parallel decreases in hippocampal astrocyte size. Similarly, GFAP area fraction in the cortex and hippocampus was significantly lower in PBM-treated AD mice than in non-PBM-treated AD mice, particularly in the cortex (Fig. 5C and D).

To distinguish neurotoxic A1 astrocytes from neuroprotective A2 subtypes, we analyzed C3 (A1 marker) and S100A10 (A2 marker) expression[49]. Immunostaining for S100A10 and C3 astrocytes revealed absent C3 expression in the WT group but was markedly elevated levels in the AD group, which were significantly decreased by PBM treatment (Fig. 5G, H, J and K). These findings were corroborated by western blot and RT-PCR analyses, which confirmed reduced C3 protein and transcript levels following photobiomodulation (Fig. 5E, F, and Supplementary Fig. 10A, B). In contrast, S100A10 expression remained relatively preserved, indicating selective suppression of the neurotoxic A1 astrocyte program. Notably, immunostaining analysis revealed a positive correlation between C3 levels and Aβ load (cortex: $r = 0.78$, $P < 0.0001$; hippocampus: $r = 0.90$, $P < 0.0001$; Fig. 5I, L). Additionally, C3 expression was positively correlated with the

diameter of microglial cell bodies (cortex: $r = 0.65$, $P < 0.001$; hippocampus: $r = 0.83$, $P < 0.0001$; Supplementary Fig. 10C and D), supporting a microglia-astrocyte signaling axis in AD progression. Together, these results indicate that photobiomodulation selectively attenuates microglia-associated A1 astrocyte activation, thereby alleviating a key astrocytic contributor to AD-associated neuroinflammation.

PBM suppresses microglial NLRP3 to limit $CD8^+$ T cell infiltration and A1 astrocyte induction

Inflammasome activation plays a critical role in regulating microglial function[50]. Based on the reduction of ASC-Aβ complexes and enhanced meningeal lymphatic drainage observed after PBM treatment, we hypothesized that PBM attenuates Aβ-driven neuroinflammation by suppressing NLRP3 inflammasome signaling in microglia. To test the requirement of microglial NLRP3, APP/PS1 and 3×Tg mice were engineered to overexpress NLRP3 selectively in microglia and subsequently subjected to PBM stimulation (Fig. 6). This strategy allowed us to determine whether forced maintenance of microglial NLRP3 signaling could counteract the beneficial effects of PBM. In both AD models, PBM markedly reduced $Iba1^+/iNOS^+$ microglial activation, suppressed A1 astrocyte-associated transcriptional programs (including C3, Gbp2, and Psmb8), decreased $GFAP^+/C3^+$ astrocytes and $CD8^+$ T cell infiltration alongside restoration of PSD-95 expression (Fig. 6B and C, Supplementary Fig. 11B-E). However, microglial NLRP3 overexpression abolished protective effects of PBM, including reductions in pro-inflammatory TIC cytokines (TNF-α, IL-1α, C1q), indicating that suppression of microglial NLRP3 signaling is a key mediator of PBM-induced neuroimmune and neuroprotective benefits (Fig. 6D-I).

To further assess whether the protective effects of PBM are consistent with pharmacological inhibition of NLRP3 inflammasome signaling, we included MCC950 as a positive control in APP/PS1 and 3×Tg mice. As expected, pharmacological inhibition of NLRP3 with MCC950 largely phenocopied the effects of PBM, rescuing cognitive deficits (Fig. 7A-F and Supplementary Fig. 12A-J), suppressing microglial and astrocytic activation, reducing $CD8^+$ T cell infiltration and restoring PSD-95 expression (Fig. 7G, H and Supplementary Fig. 12K-M), without affecting locomotor activity. These findings identify NLRP3 inflammasome signaling as a central mechanistic node linking photobiomodulation to reduced neuroinflammation.

To determine whether microglial NLRP3 directly contributes to the induction of A1 astrocyte states, we performed *in vitro* experiments using BV2 microglial cells treated with $A\beta_{1-42}$ (4 μM), the NLRP3 inhibitor MCC950, or PBM. The conditioned medium from BV2 cells (BCM) was then collected and used to culture primary astrocytes, allowing us to test whether PBM-dependent changes in the microglial secretory profile are sufficient to influence astrocyte reactivity. TIC content in the BCM of each treatment group was analyzed via ELISA, while the activation states of BV2 cells were assessed based on morphological changes (spindle-shaped resting cells vs. amoeboid activated cells). The neurotoxic ($C3^+$) and neurotrophic ($S100A10^+$) astrocytes was evaluated using immunofluorescence. Our results showed that $A\beta_{1-42}$ induced a significant activation of BV2 cells, characterized by an increased number of amoeboid microglia. However, both PBM treatment and MCC950 effectively attenuated this response, reducing the proportion of amoeboid BV2 cells (Fig. 7I, J). ELISA analysis (Fig. 7K-M) demonstrated that compared to the $A\beta_{1-42}$-only group, both PBM and MCC950 treatments strongly suppressed TIC release by BV2 cells. Importantly, BCM from these groups induced significantly fewer C3-positive astrocytes compared to the $A\beta_{1-42}$-only group (Fig. 7N), supporting the hypothesis that PBM reduces TIC, derived from microglia as key drivers of A1 astrocyte polarization, thereby modulating astrocyte morphology and C3 expression. Western blot analysis further confirmed that both PBM and MCC950 markedly suppressed the expression of NLRP3 and iNOS in BV2 cells (Fig. 7P). Moreover, immunoblotting of astrocytes cultured with BV2-derived BCM revealed that PBM significantly inhibited C3 expression, which is associated with the neurotoxic phenotype, and promoted morphological changes consistent with a homeostatic state. This *in vitro* evidence aligns with our *in vivo* results, further supporting the conclusion that PBM treatment mitigates neuroinflammation by modulating microglia-astrocyte interactions.

Finally, PBM treatment restored meningeal lymphatic vessel structure and drainage capacity, reduced $CD8^+$ T cell accumulation along mLVs and enhanced cerebrospinal fluid clearance to cervical lymph nodes, further supporting a role for PBM in reshaping central-peripheral immune trafficking (Supplementary Fig. 13).

The coordinated reduction in glial inflammasome activity and TIC cytokines highlights PBM's dual capacity to: Directly inhibit NLRP3-ASC complex assembly, curtailing IL-1β/IL-18 releases; Indirectly enhance Aβ clearance via restored mLVs function, mitigating microglial priming. This multimodal action disrupts the self-reinforcing loop of neuroinflammation-where

Aβ-driven NLRP3 activation promotes T cell recruitment and A1 astrocytes, which in turn exacerbate Aβ deposition.

Discussion

In this study, PBM was innovatively applied to inhibit activation of microglial NLRP3 inflammasome in AD, and its impact on central-peripheral immune crosstalk, reduction of ASC-dependent Aβ seeding, alleviation of chronic neuroinflammation, relief of neuronal damage, and improvement of cognitive function in AD. Specifically, we demonstrated PBM significantly reduced pro-inflammatory microglia activation in APP/PS1 and 3×Tg AD mice by suppressing Aβ-induced NLRP3 activation. Moreover, the transendothelial migration of $CD8^+$ T cells rescued by PBM is achieved by reducing the expression of VCAM1 and ICAM1 in brain vascular endothelial cells, which are mainly regulated by microglia-derived TNF-α. Notably, the accumulation of $CD8^+$ T cells in the brain is positively correlated with pro-inflammatory microglia and cognitive deficits in AD mice, highlighting the role of PBM in ameliorating cognitive impairments through the suppression of $CD8^+$ T cell recruitment. A reduction in pro-inflammatory microglia activation was accompanied by a significant decrease in TIC secretion, leading to a downregulation of TIC-dependent activation of neurotoxic reactive astrocytes (A1). Overall, our findings suggest that PBM reduce Aβ load and thus ameliorate cognition abilities through modulation of central-peripheral immune crosstalk. Importantly, additional follow-up experiments indicated that the beneficial effects of PBM on cognition and AD-related pathology were still detectable after treatment cessation, suggesting a sustained benefit beyond the immediate treatment window (Supplementary Fig. 14). Future studies with additional independent time points are needed to determine the complete duration of the effect. Therefore, photobiomodulation may represent a promising non-invasive candidate therapeutic strategy for AD that warrants further translational and clinical investigation.

While our data establish NLRP3 as a key target of PBM therapy, the precise molecular mechanisms underlying its direct inhibition remain to be fully elucidated. One plausible hypothesis center on PBM-mediated modulation of mitochondrial reactive oxygen species (mtROS)[51], a critical activator of NLRP3 inflammasome assembly[52,53]. In AD models, Aβ oligomers induce

mtROS bursts that promote NLRP3-ASC oligomerization and subsequent Caspase-1 activation[54], suggesting that the reduction in NLRP3 signaling observed here may at least partly arise from PBM-induced normalization of mitochondrial and metabolic stress. PBM therapy may counteract this by upregulating antioxidant enzymes (e.g., SOD2) or restoring mitochondrial membrane potential, thereby disrupting the redox-sensitive NLRP3 activation loop. Alternatively, PBM might directly interfere with NLRP3 inflammasome priming or assembly. Importantly, the mechanisms implicated in our previous and current studies may be mechanistically connected rather than separate. In our previous study, we found that PBM treatment can activate the cAMP/PKA signaling pathway[34], whereas the present study identifies suppression of microglial NLRP3 inflammasome activation as a central node linking PBM treatment to reduced TIC release, decreased endothelial activation, diminished $CD8^+$ T-cell recruitment, and attenuated A1-like astrocyte induction. Accumulating evidence indicates that cAMP/PKA-related signaling can negatively regulate NLRP3 inflammasome activation[55,56], and that sirtuins, particularly SIRT1, can restrain inflammatory priming through suppression of NF-κB activity, improvement of mitochondrial homeostasis, and attenuation of oxidative stress[57]. From this perspective, PBM-induced activation of cAMP/PKA-SIRT1-related signaling may function upstream of microglial NLRP3 inhibition, thereby integrating metabolic signaling, inflammasome control, and central-peripheral immune crosstalk into a unified mechanistic framework. A plausible integrated model is therefore that PBM first modulates cellular bioenergetics and second-messenger signaling, including cAMP/PKA and sirtuin-dependent pathways, which in turn reduce Aβ-associated mitochondrial stress, restore redox homeostasis, and attenuate inflammatory priming in microglia. This would be expected to limit NLRP3 inflammasome assembly and downstream release of IL-1β/IL-18 as well as TIC factors, thereby attenuating endothelial VCAM1/ICAM1 upregulation, chemokine-dependent $CD8^+$ T-cell recruitment, and induction of neurotoxic A1-like astrocytes. Such a framework is consistent with our current results as well as with prior reports showing that PBM affects mitochondrial and inflammatory regulation at multiple levels in AD-related systems. However, we acknowledge that the present study does not directly dissect each upstream signaling step in this cascade. Future studies combining pathway-specific pharmacological or genetic perturbation will be required to determine the relative contribution of cAMP/PKA, SIRT1, and mitochondrial redox regulation to NLRP3 inhibition *in vivo*.

An additional framework that may help interpret the anti-inflammatory effects of PBM is microglial immunometabolism. Pro-inflammatory microglial states are commonly associated with enhanced glycolysis, whereas more homeostatic or reparative states rely more on oxidative phosphorylation or greater metabolic flexibility[58]. In AD-related settings, Aβ has been shown to drive metabolic reprogramming of microglia from oxidative phosphorylation toward glycolysis[59], and more recent work further demonstrated that Aβ can activate the NLRP3 inflammasome by affecting microglial immunometabolism through the Syk-AMPK pathway[54]. In addition, the relationship between inflammasome signaling and glycolytic reprogramming may be bidirectional, as previous work in macrophages showed that NLRP3 activation can itself enhance glycolysis through IL-1β-dependent upregulation of PFKFB3[60]. Within this framework, PBM may act upstream by restoring mitochondrial function and redox balance and by shifting Aβ-stimulated pro-inflammatory microglia away from a glycolysis-associated state toward mitochondrial activity, as has been reported for near-infrared light[61,62]. Although we did not directly measure microglial metabolic flux in the present study, this framework is compatible with our observation that PBM suppressed microglial NLRP3 activation and downstream neuroimmune crosstalk. Thus, NLRP3-centered neuroimmune crosstalk may represent one downstream consequence of a broader PBM-associated metabolic and inflammatory reprogramming of microglia.

Although the CNS has traditionally been considered an immune-privileged organ due to limited monitoring of peripheral immune cells within the BBB and brain parenchyma, chronic neuroinflammation in AD disrupts this balance. Emerging evidence suggests that peripheral immune cells infiltrate the CNS and accumulate near pathological areas[43]. For instance, $CD8^+$ T cells and natural killer cells have been reported to accumulate in the brain of AD patients. Microglia stimulation by Aβ plaques in transgenic mouse models or $A\beta_{1\text{-}42}$ oligomers injection triggers the release of proinflammatory cytokines such as IL-1β and TNF-α, which in turn induce production of chemokine by endothelial cells[63,64]. In our study, we observed a considerable increase of $CD8^+$ T cells in the cerebral cortex of AD mice using immunofluorescence. Accumulation of $CD8^+$ T cells drives axon degeneration in the normal aging mouse CNS and contributes to age-related cognitive and motor decline[13]. Consistently, we found that the recovery of dendritic spine density induced by PBM was associated with reduced brain infiltration of $CD8^+$ T cells, suggesting a complex regulatory crosstalk among microglia, astrocytes, and T lymphocytes. Furthermore, our data showed that microglia and infiltrating T cells release

cytokines, such as CCL2, CCL3, CCL4, and CCL8, which broadly impact brain immune microenvironment homeostasis. Other studies on rodent models have shown that T cells, upon entering the brain, can alter microglia phenotypes by secreting IFN-γ, increasing microglial motility and phagocytic activity[65]. Whether these mechanisms are regulated by PBM and how they manifest in AD patients remain open questions and are central to our future research.

These findings should also be interpreted in the context of previous studies showing that Aβ oligomers can impair cognition through inflammation-related mechanisms in addition to direct synaptic toxicity. In an acute mouse model, Balducci et al. demonstrated that Aβ oligomer-induced memory impairment depends on TLR4-mediated glial activation and can be prevented by anti-inflammatory treatment, supporting a direct contribution of glial inflammatory signaling to oligomer-driven cognitive dysfunction[66]. More recently, Forloni and colleagues further expanded this framework by emphasizing the broader interplay among oligomer toxicity, inflammation, and receptor-mediated signaling, including the possible contribution of prion protein-related mechanisms[67]. There is growing evidence of TLR-4 as the mediator of the inflammatory mechanism in AD experimental models associated with Aβ[68]. Aggregated Aβ binds to TLR-4 and activates microglia, resulting in increased phagocytosis and cytokine production. Inflammatory factors including TNF-α, interleukin 1β and interleukin 6 are under the nuclear factor kappa B (NFκB) transcription factor sensitive to TLR4-activation through a MyD88 dependent and independent pathway[69]. In addition, the stimulation of TLRs has been proven to be part of the activation of the NLRP3 inflammasome[68,70]. Clinical data and animal studies indicate that Aβ deposits can cause inflammasome activation[71]. Primary microglial cells were treated with AβOs and NLRP3 inflammasome activation, was determined by Caspase1 cleavage, and IL-1β production[72]. Therefore, accumulating evidence indicates that Aβ can engage TLR4/NF-κB signaling and that oligomeric Aβ species are capable of activating the NLRP3 inflammasome in microglia, providing a mechanistic bridge between oligomer-triggered innate immune sensing and downstream inflammatory amplification. In this work, we found that, in chronic transgenic AD models, Aβ-/oligomer-associated inflammatory signaling may converge on a microglial NLRP3-centered neuroimmune cascade involving TIC release, endothelial activation, $CD8^+$ T-cell recruitment, and A1-like astrocyte induction. In this sense, the present study may add a central-peripheral immune crosstalk dimension to the emerging concept.

Alzheimer's disease is characterized by a complex interplay of Aβ accumulation, tauopathy, chronic neuroinflammation, vascular dysfunction, and disrupted central-peripheral immune communication, necessitating therapeutic strategies that that can act across multiple pathological levels rather than on a single molecular target [73]. Our findings reveal that while MCC950, a selective NLRP3 inhibitor, and transcranial PBM therapy both attenuate neuroinflammation in AD models by suppressing NLRP3 inflammasome activity, photobiomodulation exerts broader multimodal effects that address the multifactorial pathology of AD. Unlike MCC950, which solely targets NLRP3 assembly, PBM therapy concurrently enhances Aβ clearance via mLVs repair (improved OVA-A647 drainage), normalizes vascular endothelial adhesion molecules, and restores microglial homeostasis-effects unattainable through pharmacological NLRP3 inhibition alone. These effects collectively disrupt the self-reinforcing neuroinflammatory loop where Aβ deposition activates NLRP3 inflammasomes, which in turn promote chemokine-driven T cell infiltration and neurotoxic astrocyte polarization. The non-pharmacological nature of PBM therapy further circumvents challenges inherent to drug-based interventions, such as blood-brain barrier penetration limitations, systemic toxicity, and off-target effects. Utilize the pleiotropic mechanisms of photobiological regulation, including mitochondrial redox balance restoration[74], glymphatic clearance potentiation[32], and innate immune reprogramming-PBM therapy offers a scalable and sustainable approach for long-term AD management.

Recent clinical trials using transcranial near-infrared light (NIR) in healthy adults reported improved visual working memory capacity[75], underscoring its translational promise. From a translational perspective, the therapeutic relevance of photobiomodulation lies not only in its non-invasive nature, but also in its apparent ability to influence multiple interacting pathological processes that are highly relevant to AD. In the present study, PBM did not merely alter a single inflammatory readout; rather, it concurrently reduced microglial NLRP3 activation, TIC release, endothelial adhesion molecule upregulation, $CD8^+$ T-cell recruitment, and A1-like astrocyte induction, while improving cognition in two independent AD models. This multi-level action is particularly important in AD, where the limited success of many therapeutic approaches may reflect the difficulty of targeting a disease driven by convergent amyloid, inflammatory, vascular, and immune-trafficking abnormalities rather than by a single molecular lesion. In this context, photobiomodulation may represent a mechanistically supported non-invasive candidate therapeutic strategy for AD, especially as an approach aimed at neuroimmune rebalancing in

addition to amyloid-related pathology. At the same time, the concept of PBM therapy as a practical therapeutic strategy should be interpreted with appropriate caution[76]. Although preclinical work and early human studies suggest that transcranial photobiomodulation is feasible and may improve selected cognitive or network-level outcomes[75,77,78], the field still faces several important translational challenges, including optimization of wavelength, irradiance, treatment duration and frequency, tissue dosimetry, identification of target-engagement biomarkers, and validation in larger sham-controlled clinical cohorts. In addition, it remains necessary to define the therapeutic window, the durability of benefit, and the patient populations most likely to respond. Thus, our findings support photobiomodulation not as a clinically established therapy, but as a promising translational direction that merits further mechanistic and clinical development.

This study underscores the potential of PBM as a feasible, non-invasive therapeutic approach for AD, primarily by alleviating NLRP3-dependent chronic neuroinflammation (Supplementary Fig. 15). Our findings highlight the critical role of chronic inflammation in AD pathogenesis and brain-related diseases. However, further research is needed to unravel the underlying mechanisms, refine PBM treatment protocols, and evaluate its clinical translational potential. Nevertheless, the results of this study provide a promising basis for future investigations into the use of PBM as a non-invasive and drug-free treatment for AD.

Data availability

All data needed to evaluate the conclusions in the paper are present in the paper and/or the Supplementary Information. Due to space limitations, detailed descriptions of materials and methods are provided in the Supplementary material. Additional data related to this paper may be requested from the authors.

Acknowledgements

We thank all authors for their kind participation in this study. The thumbnail image for the online table of contents was created in BioRender. Qi, S. (2026) https://BioRender.com/oxjlo88.

Funding

This work was supported by the STI2030-Major Projects (2022ZD0212200), National Natural Science Foundation of China (62305119; 62335007), the Natural Science Foundation of Guangdong Province, China (2023A1515011489; 2025A1515011522), Science and Technology Plan Project of Guangzhou, China (202201010291), China Postdoctoral Science Foundation (2022M721221), and the Youth Science and Technology Talent Cultivation Program of Guangdong Science and Technology Association, China (SKXRC2025015).

Competing interests

The authors declare that they have no competing interests.

Supplementary material

Supplementary material is available at *Brain* online.

References

1. Lau S-F, Wu W, Wong HY, et al. The VCAM1-ApoE pathway directs microglial chemotaxis and alleviates Alzheimer's disease pathology. *Nature Aging*. 2023;3(10):1219-1236.

2. Porsteinsson AP, Isaacson RS, Knox S, Sabbagh MN, Rubino I. Diagnosis of early Alzheimer's disease: Clinical practice in 2021. *J Prev Alzheimers Dis*. 2021;8(3):371-386.

3. Leng F, Edison P. Neuroinflammation and microglial activation in Alzheimer disease: Where do we go from here? *Nat Rev Neurol*. 2021;17(3):157-172.

4. Morris G, Berk M, Maes M, Puri BK. Could Alzheimer's disease originate in the periphery and if so how so? *Mol Neurobiol*. 2019;56(1):406-434.

5. Bettcher BM, Tansey MG, Dorothée G, Heneka MT. Peripheral and central immune system crosstalk in Alzheimer disease - a research prospectus. *Nat Rev Neurol*. 2021;17(11):689-701.

6. Cao W, Zheng H. Peripheral immune system in aging and Alzheimer's disease. *Mol Neurodegener*. 2018;13:51.

7. Le Page A, Dupuis G, Frost EH, et al. Role of the peripheral innate immune system in the development of Alzheimer's disease. *Exp Gerontol*. 2018;107:59-66.

8. Webers A, Heneka MT, Gleeson PA. The role of innate immune responses and neuroinflammation in amyloid accumulation and progression of Alzheimer's disease. *Immunol Cell Biol*. 2020;98(1):28-41.

9. Saijo K, Winner B, Carson CT, et al. A Nurr1/CoREST pathway in microglia and astrocytes protects dopaminergic neurons from inflammation-induced death. *Cell*. 2009;137(1):47-59.

10. Heneka MT, McManus RM, Latz E. Inflammasome signaling in brain function and neurodegenerative disease. *Nat Rev Neurosci*. 2018;19(10):610-621.

11. Jorfi M, Maaser-Hecker A, Tanzi RE. The neuroimmune axis of Alzheimer's disease. *Genome Med*. 2023;15(1):6.

12. Groh J, Knöpper K, Arampatzi P, et al. Accumulation of cytotoxic T cells in the aged CNS leads to axon degeneration and contributes to cognitive and motor decline. *Nat Aging*. 2021;1(4):357-367.

13. Jorfi M, Park J, Hall CK, et al. Infiltrating CD8+ T cells exacerbate Alzheimer's disease pathology in a 3D human neuroimmune axis model. *Nat Neurosci*. 2023;26(9):1489-1504.

14. Su W, Saravia J, Risch I, et al. CXCR6 orchestrates brain CD8 T cell residency and limits mouse Alzheimer's disease pathology. *Nat Immunol*. 2023;24(10):1735.

15. Marsh SE, Abud EM, Lakatos A, et al. The adaptive immune system restrains Alzheimer's disease pathogenesis by modulating microglial function. *PNAS*. 2016;113(9):E1316-E1325.

16. Kim K, Wang X, Ragonnaud E, et al. Therapeutic B-cell depletion reverses progression of Alzheimer's disease. *Nat Commun*. 2021;12(1):2185.

17. Chen XY, Firulyova M, Manis M, et al. Microglia-mediated T cell infiltration drives neurodegeneration in tauopathy. *Nature*. 2023;615(7953):668-677.

18. Aspelund A, Antila S, Proulx ST, et al. A dural lymphatic vascular system that drains brain interstitial fluid and macromolecules. *J Exp Med*. 2015;212(7):991-999.

19. Louveau A, Smirnov I, Keyes TJ, et al. Structural and functional features of central nervous system lymphatic vessels. *Nature*. 2015;523(7560):337.

20. Da Mesquita S, Papadopoulos Z, Dykstra T, et al. Meningeal lymphatics affect microglia responses and anti-Aβ immunotherapy. *Nature*. 2021;593(7858):255.

21. Shechter R, Miller O, Yovel G, et al. Recruitment of beneficial M2 macrophages to injured spinal cord Is orchestrated by remote brain choroid plexus. *Immunity*. 2013;38(3):555-569.

22. Cugurra A, Mamuladze T, Rustenhoven J, et al. Skull and vertebral bone marrow are myeloid cell reservoirs for the meninges and CNS parenchyma. *Science*. 2021;373(6553):409.

23. Sweeney MD, Sagare AP, Zlokovic BV. Blood-brain barrier breakdown in Alzheimer disease and other neurodegenerative disorders. *Nat Rev Neurol*. 2018;14(3):133-150.

24. Herisson F, Frodermann V, Courties G, et al. Direct vascular channels connect skull bone marrow and the brain surface enabling myeloid cell migration. *Nat Neurosci*. 2018;21(9):1209.

25. Sweeney MD, Zhao Z, Montagne A, Nelson AR, Zlokovic BV. Blood-brain barrier: From physiology to disease and back. *Physiol Rev*. 2019;99(1):21-78.

26. Mason HD, McGavern DB. How the immune system shapes neurodegenerative diseases. *Trends Neurosci*. 2022;45(10):733-748.

27. Wilson EH, Weninger W, Hunter CA. Trafficking of immune cells in the central nervous system. *J Clin Invest*. 2010;120(5):1368-1379.

28. Togo T, Akiyama H, Iseki E, et al. Occurrence of T cells in the brain of Alzheimer's disease and other neurological diseases. *J Neuroimmunol*. 2002;124(1-2):83-92.

29. Gate D, Saligrama N, Leventhal O, et al. Clonally expanded CD8 T cells patrol the cerebrospinal fluid in Alzheimer's disease. *Nature*. 2020;577(7790):399.

30. Murdock MH, Yang CY, Sun N, et al. Multisensory gamma stimulation promotes glymphatic clearance of amyloid. *Nature*. 2024;627:149-156.

31. Tao L, Liu Q, Zhang F, et al. Microglia modulation with 1070-nm light attenuates Aβ burden and cognitive impairment in Alzheimer's disease mouse model. *Light Sci Appl*. 2021;10(1):179.

32. Wang M, Yan C, Li X, et al. Non-invasive modulation of meningeal lymphatics ameliorates ageing and Alzheimer's disease-associated pathology and cognition in mice. *Nat Commun*. 2024;15(1):1453.

33. Shen Q, Liu L, Gu X, Xing D. Photobiomodulation suppresses JNK3 by activation of ERK/MKP7 to attenuate AMPA receptor endocytosis in Alzheimer's disease. *Aging Cell*. 2021;20(1):e13289.

34. Zhang Z, Shen Q, Wu XL, Zhang D, Xing D. Activation of PKA/SIRT1 signaling pathway by photobiomodulation therapy reduces Aβ levels in Alzheimer's disease models. *Aging Cell*. 2020;19(1):e13054

35. Heneka MT, Kummer MP, Latz E. Innate immune activation in neurodegenerative disease. *Nat Rev Immunol*. 2014;14(7):463-77.

36. Tzioras M, McGeachan RI, Durrant CS, Spires-Jones TL. Synaptic degeneration in Alzheimer disease. *Nat Rev Neurol*. 2023;19(1):19-38.

37. Park JS, Kam TI, Lee S, et al. Blocking microglial activation of reactive astrocytes is neuroprotective in models of Alzheimer's disease. *Acta Neuropathol Commun*. 2021;9(1):78.

38. Hu D, Xia W, Weiner HL. CD8(+) T cells in neurodegeneration: Friend or foe? *Mol Neurodegener*. 2022;17(1):59.

39. Wang P, Yao L, Luo M, et al. Single-cell transcriptome and TCR profiling reveal activated and expanded T cell populations in Parkinson's disease. *Cell Discov*. 2021;7(1):52.

40. Marchetti L, Engelhardt B. Immune cell trafficking across the blood-brain barrier in the absence and presence of neuroinflammation. *Vasc Biol*. 2020;2(1):1-18.

41. Joly-Amado A, Hunter J, Quadri Z, et al. CCL2 overexpression in the brain promotes glial activation and accelerates tau pathology in a mouse model of tauopathy. *Front Immunol*. 2020;11:997.

42. Shi Z, Yu P, Lin W-J, et al. Microglia drive transient insult-induced brain injury by chemotactic recruitment of CD8+ T lymphocytes. *Neuron*. 2023;111(5):696-710.e9.

43. Unger MS, Li E, Scharnagl L, et al. CD8+ T-cells infiltrate Alzheimer's disease brains and regulate neuronal- and synapse-related gene expression in APP-PS1 transgenic mice. *Brain Behav Immun*. 2020;89:67-86.

44. Zhang X, Wang R, Chen H, et al. Aged microglia promote peripheral T cell infiltration by reprogramming the microenvironment of neurogenic niches. *Immun Ageing*. 2022;19(1):34.

45. Wang Q, Yao H, Liu W, et al. Microglia polarization in Alzheimer's disease: Mechanisms and a potential therapeutic target. *Front Aging Neurosci*. 2021;13:772717.

46. Tang Y, Le W. Differential roles of M1 and M2 microglia in neurodegenerative diseases. *Mol Neurobiol*. 2016;53(2):1181-1194.

47. Wang X, Li X, Zuo X, et al. Photobiomodulation inhibits the activation of neurotoxic microglia and astrocytes by inhibiting Lcn2/JAK2-STAT3 crosstalk after spinal cord injury in male rats. *J Neuroinflammation*. 2021;18(1):256.

48. Escartin C, Galea E, Lakatos A, et al. Reactive astrocyte nomenclature, definitions, and future directions. *Nat Neurosci*. 2021;24(3):312-325.

49. Li S, Fang Y, Zhang Y, et al. Microglial NLRP3 inflammasome activates neurotoxic astrocytes in depression-like mice. *Cell Rep*. 2022;41(4):111532.

50. Xu L, He D, Bai Y. Microglia-mediated inflammation and neurodegenerative disease. *Mol Neurobiol*. 2016;53(10):6709-6715.

51. Huang ZH, Hamblin MR, Zhang QG. Photobiomodulation in experimental models of Alzheimer's disease: State-of-the-art and translational perspectives. *Alzheimers Res Ther*. 2024;16(1):114.

52. Billingham LK, Stoolman JS, Vasan K, et al. Mitochondrial electron transport chain is necessary for NLRP3 inflammasome activation. *Nature Immunology*. 2022;23(5):692-704.

53. Casey AM, Ryan DG, Prag HA, et al. Pro-inflammatory macrophages produce mitochondria-derived superoxide by reverse electron transport at complex I that regulates IL-1β release during NLRP3 inflammasome activation. *Nat Metab*. 2025; 7(3):493-507.

54. Jung ES, Suh K, Han JH, et al. Amyloid-β activates NLRP3 inflammasomes by affecting microglial immunometabolism through the Syk-AMPK pathway. *Aging Cell*. 2022;21(5):e13623.

55. Tang TT, Gong T, Jiang W, Zhou RB. GPCRs in NLRP3 inflammasome activation, regulation, and therapeutics. *Trends Pharmacol Sci*. 2018;39(9):798-811.

56. Yan YQ, Jiang W, Liu L, et al. Dopamine controls systemic inflammation through inhibition of NLRP3 inflammasome. *Cell*. 2015;160(1-2):62-73.

57. Fernando KKM, Wijayasinghe YS. Sirtuins as potential therapeutic targets for mitigating neuroinflammation associated with Alzheimer's disease. *Front Cell Neurosci*. 2021;15:746631.

58. Jung ES, Choi H, Mook-Jung I. Decoding microglial immunometabolism: A new frontier in Alzheimer's disease research. *Mol Neurodegener*. 2025;20(1):37.

59. Baik SH, Kang S, Lee W, et al. A breakdown in metabolic reprogramming causes microglia dysfunction in Alzheimer's disease. *Cell Metab*. 2019;30(3):493-507 e6.

60. Finucane OM, Sugrue J, Rubio-Araiz A, Guillot-Sestier MV, Lynch MA. The NLRP3 inflammasome modulates glycolysis by increasing PFKFB3 in an IL-1beta-dependent manner in macrophages. *Sci Rep*. 2019;9(1):4034.

61. Stepanov YV, Golovynska I, Zhang R, et al. Near-infrared light reduces beta-amyloid-stimulated microglial toxicity and enhances survival of neurons: mechanisms of light therapy for Alzheimer's disease. *Alzheimers Res Ther*. 2022;14(1):84.

62. Hamblin MR. Transcranial photobiomodulation for the brain: A wide range of clinical applications. *Neural Regen Res*. 2024;19(3):483-484.

63. Zhang W, Smith C, Howlett C, Stanimirovic D. Inflammatory activation of human brain endothelial cells by hypoxic astrocytes in vitro is mediated by IL-1β. *J Cereb Blood Flow Metab*. 2000;20(6):967-978.

64. Eisenhauer PB, Jacewicz MS, Conn KJ, et al. Escherichia coli Shiga toxin 1 and TNF-α induce cytokine release by human cerebral microvascular endothelial cells. *Microb Pathog*. 2004;36(4):189-196.

65. Fisher Y, Nemirovsky A, Baron R, Monsonego A. T cells specifically targeted to amyloid plaques enhance plaque clearance in a mouse model of Alzheimer's disease. *PLOS ONE*. 2010;5(5):e10830.

66. Balducci C, Frasca A, Zotti M, et al. Toll-like receptor 4-dependent glial cell activation mediates the impairment in memory establishment induced by β-amyloid oligomers in an acute mouse model of Alzheimer's disease. *Brain Behav Immun*. 2017;60:188-197.

67. Forloni G, La Vitola P, Balducci C. , Oligomeropathies, inflammation and prion protein binding. *Front Neurosci*. 2022;16:822420.

68. Liu Y, Dai Y, Li Q, et al. Beta-amyloid activates NLRP3 inflammasome via TLR4 in mouse microglia. *Neurosci Lett*. 2020;736.

69. Hughes C, Choi ML, Yi JH, et al. Beta amyloid aggregates induce sensitised TLR4 signaling causing long-term potentiation deficit and rat neuronal cell death. *Commun Biol*. 2020;3(1).

70. Li YF, Chen XJ, Zhou ML, Feng SF, Peng XP, Wang Y. Microglial TLR4/NLRP3 inflammasome signaling in Alzheimer's disease. *J Alzheimers Dis*. 2024;97(1):75-88.

71. Guan YD, Han F. Key mechanisms and potential targets of the NLRP3 inflammasome in neurodegenerative diseases. *Front Integr Neurosc*. 2020;14:37.

72. Luciunaite A, McManus RM, Jankunec M, et al. Soluble Aβ oligomers and protofibrils induce NLRP3 inflammasome activation in microglia. *J Neurochem*. 2020;155(6):650-661.

73. Scheltens P, De Strooper B, Kivipelto M, et al. Alzheimer's disease. *Lancet*. 2021;397(10284):1577-1590.

74. Enengl J, Hamblin MR, Dungel P. Photobiomodulation for Alzheimer's disease: Translating basic research to clinical application. *J Alzheimers Dis*. 2020;75(4):1073-1082.

75. Zhao CG, Li DW, Kong YJ, et al. Transcranial photobiomodulation enhances visual working memory capacity in humans. *Sci Adv*. 2022;8(48):eabq3211.

76. Lin H, Li DY, Zhu JT, et al. Transcranial photobiomodulation for brain diseases: Review of animal and human studies including mechanisms and emerging trends. *Neurophotonics*. 2024;11(1).

77. Saltmarche AE, Naeser MA, Ho KF, Hamblin MR, Lim L. Significant improvement in cognition in mild to moderately severe dementia cases treated with transcranial plus intranasal photobiomodulation: Case series report. *Photomed Laser Surg*. 2017;35(8):432-441.

78. Salehpour F, Hamblin MR, DiDuro JO. Rapid reversal of cognitive decline, olfactory dysfunction, and quality of life using multi-modality photobiomodulation therapy: Case report. *Photobiomod Photomed*. 2019;37(3):159-167.

Figure legends

Figure 1 Therapeutic effects of PBM on cognition and pathology in AD mice. (A) Schedule of treatments and behavior tests of APP/PS1 and 3×Tg mice. **(B)** Novel recognition index of novel object recognition (NOR) test ($n = 16$). **(C)** Spontaneous alternation behavior was measured in AD mice or WT mice with or without PBM ($n = 16$). **(D)** The percentage of freezing during fear conditioning test ($n = 16$). **(E)** Volcano plot of DEGs of 3×Tg versus 3×Tg treated with PBM. The dashed line represents $P_{adj} = 0.05$ ($n = 4$). **(F)** GO terms upon PBM treatment in 3×Tg mice ($n = 4$). **(G)** KEGG pathway enrichment upon PBM treatment in 3×Tg mice ($n = 4$). **(H)** Representative images immunofluorescent stained with Aβ and ASC specific antibodies. And the white arrows indicate the co localization positive areas of ASC and Aβ. Scale bar: 50 μm. **(I)** Quantification of area fraction of Aβ and ASC in the cerebral cortex of WT, APP/PS1 and 3×Tg mice under the treatment with or without PBM ($n = 6$). **(J)** Representative images of colocalization exists between Aβ and ASC specks is shown for maximum intensity profile in the cerebral cortex of APP/PS1 and 3×Tg mice under treatment with or without PBM. In addition, the fluorescence intensity of ASC and Aβ along the white line was analyzed to characterize their co localization. Scale bar: 20 μm. **(K)** Relative mRNA expression of Caspase-1, IL-18, IL-1β and IL-6 presented as the fold change in the cerebral cortex of WT, APP/PS1 and 3×Tg mice under treatment with or without PBM ($n = 3$). All the data are reported as mean ± SEM. $^{*}P < 0.05$, $^{**}P < 0.01$, $^{***}P < 0.001$ and

****$P < 0.0001$ versus the control group; #$P < 0.05$, ##$P < 0.01$, ###$P < 0.001$ and ####$P < 0.0001$ versus the indicated group. ns = not significant.

Figure 2 Inhibiting CD8⁺ T cell infiltration by PBM rescues neuronal damage. (A) TUNEL assay revealed apoptotic cells in the infiltration site of CD8⁺ T cells in the indicated group. Scale bar: 50 μm. **(B)** Immunofluorescence staining confirmed the expression of granzyme A in CD8⁺ T cells in the cortex of APP/PS1 and 3×Tg mice under treatment with or without PBM. Scale bar: 10 μm. **(C)** Immunofluorescence staining confirmed the expression of perforin in CD8⁺ T cells in the cortex of APP/PS1 and 3×Tg mice under treatment with or without PBM. Scale bar: 10 μm. **(D)** Quantitative analysis of TUNEL positive cells in the cortex of APP/PS1 and 3×Tg mice under the treatment with or without PBM. **(E)** Quantification of area fraction of granzyme A in the cortex of APP/PS1 and 3×Tg mice under the treatment with or without PBM (n = 7). **(F)** Quantification of area fraction of perforin in the cortex of APP/PS1 and 3×Tg mice under the treatment with or without PBM (n = 5). **(G)** The viability of primary cortical neurons was reduced 24 h after co-cultured with active CD8⁺ T cells. Neurons were subjected to $A\beta_{1-42}$ (4 μM) with or without PBM before being co-culture with CD8⁺ T cells. Cell viability was detected by CCK-8 (n = 4). **(H)** Reduced viability of primary cortical neurons cultured with medium conditioned by activated CD8⁺ T cells (CD8⁺ T CM). Neurons were subjected to $A\beta_{1-42}$ (4 μM) with or without PBM before being co-cultured with CD8⁺ T CM. Cell viability was tested for 24 h after adding a conditioned medium. Sham CM: non-conditioned medium (n = 4). **(I)** Schedule of treatments and behavior tests of AD mice with anti-CD8α/PBM (n = 5). **(J)** Representative images of brain sections of CD8⁺ T cells ablated AD mice stained with NeuN, PSD-95 and DAPI, and **(K)** quantification of area fraction of of NeuN and PSD-95, respectively (n = 5). Scale bar: 50 μm. All the data are reported as mean ± SEM. #$P < 0.05$, ##$P < 0.01$ and ###$P < 0.001$ versus the indicated group.

Figure 3 PBM treatment suppresses microglia-driven chemokine signaling to limit CD8⁺ T cell recruitment. (A) Representative images immunofluorescent stained with CD31 and VCAM1 specific antibodies. Scale bar: 50 μm. **(B)** Quantitative analysis of the area ratio of VCAM1 to CD31 in the brain of WT, APP/PS1 and 3×Tg mice under treatment with or without PBM (n = 5). **(C)** Representative images immunofluorescent stained with CD31 and ICAM1 specific antibodies. Scale bar: 50 μm. **(D)** Quantitative analysis of the area ratio of ICAM1 to CD31 in the brain of WT, APP/PS1 and 3×Tg mice under treatment with or without PBM (n = 5). **(E)** Heatmap of differentially expressed genes in cortex from 3×Tg mice treated with or without PBM. Normalized expression values are depicted (blue: low expression, red: high expression) (n = 4). **(F-G)** Quantification of TNF-α in the serum and in the cerebral cortex homogenates of WT, APP/PS1 and 3×Tg mice under treatment with or

without PBM were measured by ELISA (n = 3). **(H-I)** Quantification of C1q in the serum and in the cerebral cortex homogenates of WT, APP/PS1 and 3×Tg mice under treatment with or without PBM were measured by ELISA (n = 4). **(J)** The relative mRNA expressions of TNF-α, IL-1α, and C1q are presented as the fold change in the cerebral cortex of each group (n = 3). **(K-L)** Quantification of IL-1α in the serum and in the cerebral cortex homogenates of WT, APP/PS1 and 3×Tg mice under treatment with or without PBM were measured by ELISA (n = 3). **(M)** The relative mRNA expressions of CCL2, CCL3, CCL4 and CCL8 are presented as the fold change in the cerebral cortex of each group (n = 4). All the data are reported as mean ± SEM. $^{**}P < 0.005$, $^{***}P < 0.001$ and $^{****}P < 0.0001$ versus the WT group; $\#P < 0.05$, $\#\#P < 0.01$, $\#\#\#P < 0.001$ and $\#\#\#\#P < 0.0001$ versus the indicated group. ns = not significant.

Figure 4 PBM attenuates NLRP3-linked pro-inflammatory microglial states. (A) Representative images of immunofluorescent stained with Iba1 and iNOS specific antibodies. Scale bar: 50 μm. **(B-E)** Quantification of area fraction of Iba1 and iNOS in the cerebral cortex and hippocampus of WT, APP/PS1 and 3×Tg mice under treatment with or without PBM (n = 4). **(F)** Representative percentages of ramified and other microglial phenotypes in each group. **(G, H)** Quantification of cell body diameter of Iba1 positive cells in the cerebral cortex and hippocampus of WT, APP/PS1 and 3×Tg mice under treatment with or without PBM (n = 4 mice per group, with 6-12 cells analyzed per mouse). **(I)** The Spearman's rank correlation coefficient analysis between Aβ area fraction and diameter of Iba1 positive cells in the cerebral cortex and hippocampus of WT, APP/PS1 and 3×Tg mice under the treatment with or without PBM. **(J)** Representative western blot bands of iNOS, Iba1, NLRP3, ASC, and quantification analysis of iNOS **(K)**, Iba1 **(L)**, NLRP3 **(M)**, and ASC **(N)** in the cerebral cortex of WT, APP/PS1 and 3×Tg mice under treatment with or without PBM (n = 3). **(O, P)** Relative mRNA expression of iNOS and Iba1 presented as the fold change in the cerebral cortex of WT, APP/PS1 and 3×Tg mice under treatment with or without PBM (n = 4). **(Q)** The Spearman's rank correlation coefficient analysis between the number of $CD8^+$ T cells and diameter of Iba1 positive cells. All the data are reported as mean ± SEM. $^{*}P < 0.05$, $^{**}P < 0.01$, $^{***}P < 0.001$ and $^{****}P < 0.0001$ versus the WT group; $\#P < 0.05$, $\#\#P < 0.01$, $\#\#\#P < 0.001$ and $\#\#\#\#P < 0.0001$ versus the indicated group. ns = not significant.

Figure 5 PBM inhibits microglia-associated A1-like astrocytes activation in AD. (A) Representative immunofluorescent images of GFAP and **(B)** quantitative analysis of the soma area

(μm^2) of GFAP positive cells in the cerebral cortex and hippocampus of WT, APP/PS1 and 3×Tg mice under treatment with or without PBM (n = 4 mice per group, with 6-7 cells analyzed per mouse). Scale bar: 50 μm. **(C, D)** Quantification of GFAP area fraction in the cerebral cortex and hippocampus of each group (n = 5). **(E)** Representative western blot bands of S100A10 and C3 in the cerebral cortex of WT, APP/PS1 and 3×Tg mice under the treatment with or without PBM. **(F)** Quantitative western blot analysis of S100A10 and C3 in the cerebral cortex of WT, APP/PS1 and 3×Tg mice under the treatment with or without PBM (n = 3). **(G, J)** Representative images immunofluorescent stained with S100A10 and C3 specific antibodies and quantification of area fraction of C3 in the cortex **(H)** and hippocampus **(K)** of each group (n = 4). Scale bar: 50 μm. **(I, L)** The Spearman's rank correlation coefficient analysis between area fraction of Aβ and C3 in the cerebral cortex (I) and hippocampus (L) of WT, APP/PS1 and 3×Tg mice under the treatment with or without PBM. All the data are reported as mean ± SEM. *$P < 0.05$, **$P < 0.01$, ***$P < 0.001$ and ****$P < 0.0001$ versus the control group; #$P < 0.05$, ##$P < 0.01$, ###$P < 0.001$ and ####$P < 0.0001$ versus the indicated group. ns = not significant.

Figure 6 Overexpression of NLRP3 in microglia blocks the effects of PBM treatments. (A) The experimental timeline of AAV infusion, PBM treatment and tissue collection. **(B)** Heatmap of A1-specific astrocyte genes. Blue and red denote downregulated and upregulated genes, respectively. n = 3. *$P < 0.05$, **$P < 0.01$, ***$P < 0.001$ for comparisons between AAV2/5-hIBA1a-EGFP and PBM+AAV2/5-hIBA1a-EGFP within each genotype (APP/PS1 or 3×Tg); #$P < 0.05$, ##$P < 0.01$, ###$P < 0.001$ for comparisons between PBM+AAV2/5-hIBA1a-EGFP and PBM+AAV2/5-hIBA1a-NLRP3-EGFP within each genotype. **(C)** Representative images immunofluorescent stained with Iba1 and iNOS, GFAP and C3, CD8 and PSD-95 specific antibodies in the cortex of each group (n = 4). Nuclei were counterstained with DAPI. Scale bar: 100 μm. **(D-I)** Quantification of TNF-α, IL-1α, C1q in the cerebral cortex homogenates of each group were measured by ELISA (n = 6). All the data are reported as mean ± SEM. #$P < 0.05$, ##$P < 0.01$ and ###$P < 0.001$ versus the indicated group. ns = not significant.

Figure 7 PBM treatment interferes with the activation of NLRP3 inflammasomes in microglia, suppressing the induction of neurotoxic astrocytes. (A) Schematic of AD mice with or without MCC950/PBM for a total of 4 weeks (n = 10). **(B, D)** Object recognition index of NOR test of APP/PS1 mice (B) or 3×Tg mice (D) with or without MCC950/ PBM (n = 10). **(C, E)**

Spontaneous alternation behavior was measured in APP/PS1 mice (C) or 3×Tg mice (E) with or without MCC950/ PBM (n = 10). **(F)** Representative test paths of open field test (n = 10). **(G)** Representative images immunofluorescent stained with GFAP and C3 specific antibodies in the cortex of each group (n = 4). Scale bar: 50 μm. **(H)** Representative images immunofluorescent stained with Iba1 and iNOS specific antibodies in the cortex of each group (n = 3-4). Scale bar: 50 μm. **(I)** Representative images of morphological changes of BV2 cells after pretreatment with NLRP3 specific inhibitor MCC950 (7.5 nM), $A\beta_{1-42}$ (4 μM) or PBM, and representative immunofluorescence for S100A10 and C3 of each primary astrocyte group with BV2-conditioned medium. Scale bar: 50 μm. **(J)** Representative percentages of spindle and amoebocyte BV2 cell in each group for (i). **(K-M)** TIC levels in BV2 cells culture medium are tested via ELISA in each group (n = 4). **(N, O)** Quantification of area fraction of C3 and S100A10 of primary astrocyte in each group (n = 4). **(P)** Representative western blot bands and quantification analysis of iNOS, NLRP3, C3 and S100A10 of BV2 cell and primary astrocyte in each group. All the data are reported as mean ± SEM. *$P < 0.05$, **$P < 0.01$ and ***$P < 0.001$ versus the control group; #$P < 0.05$, ##$P < 0.01$ and ###$P < 0.001$ versus the indicated group. ns = not significant.

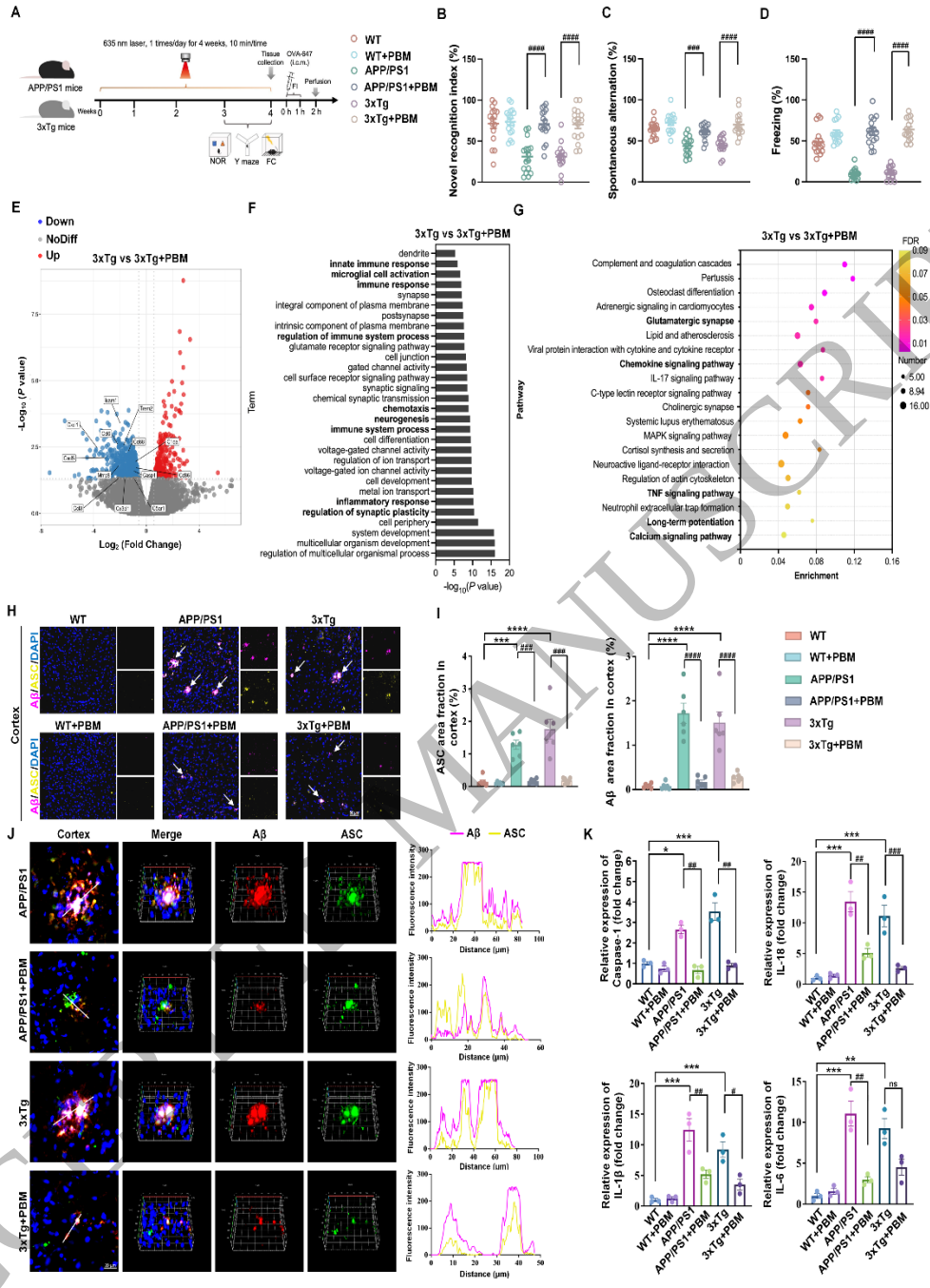

Figure 1
441x532 mm (x DPI)

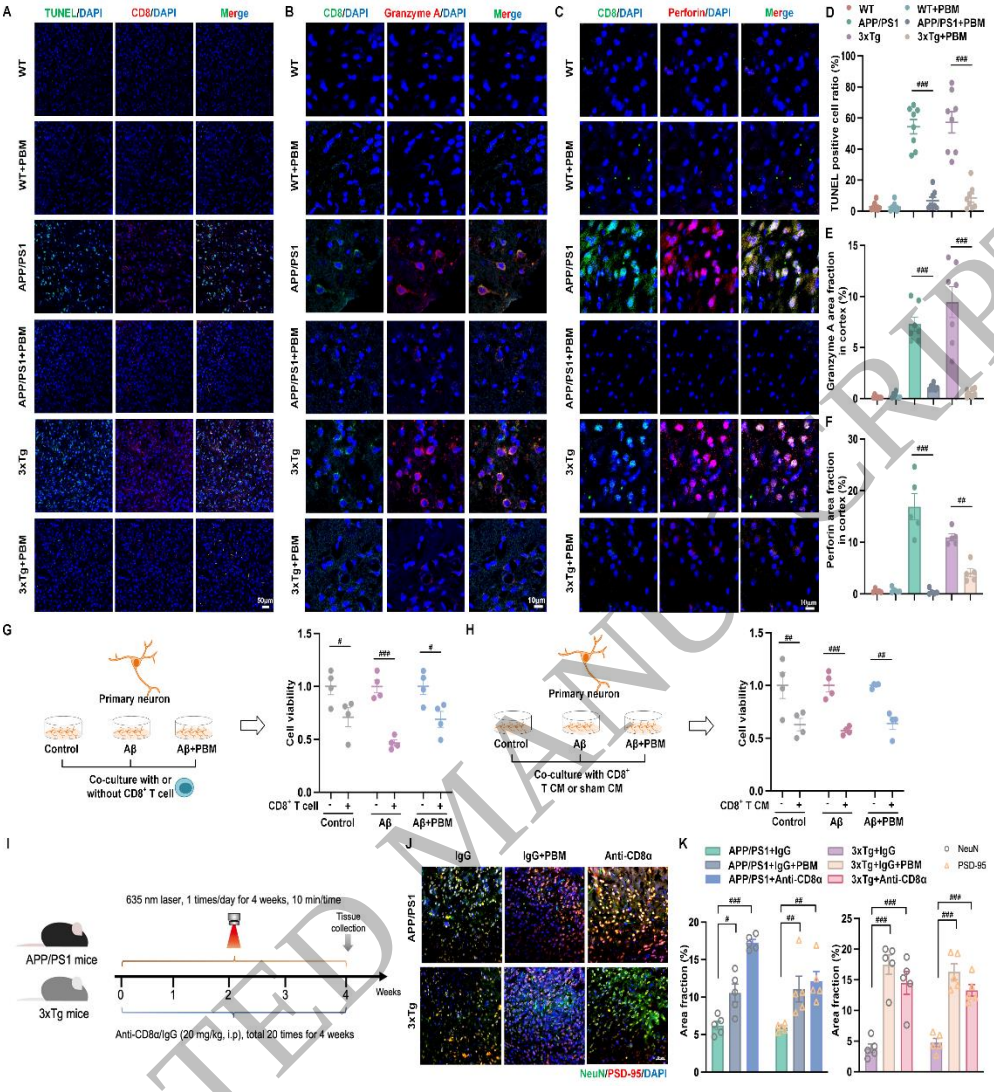

Figure 2
510x465 mm (x DPI)

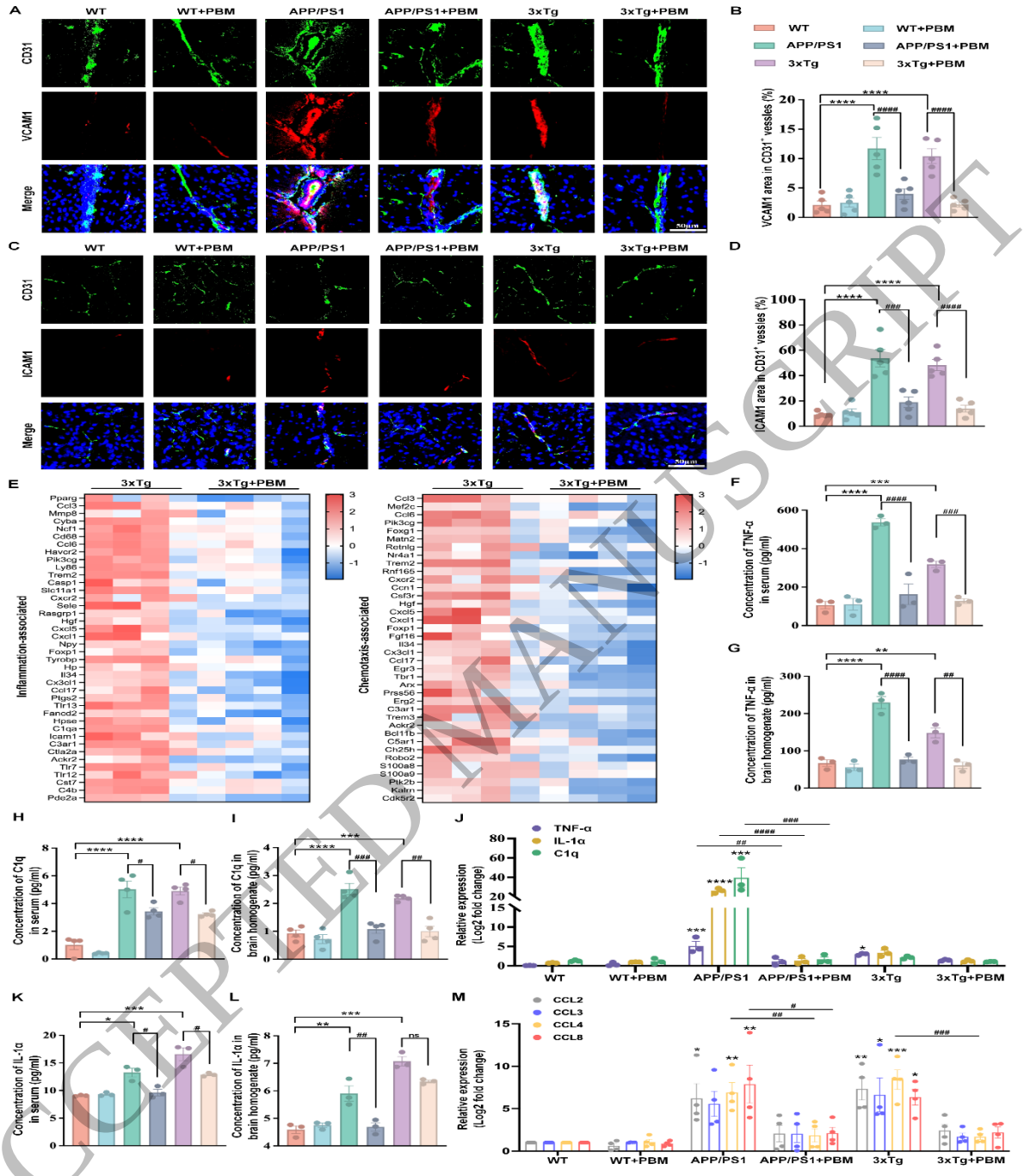

Figure 3
318x559 mm (x DPI)

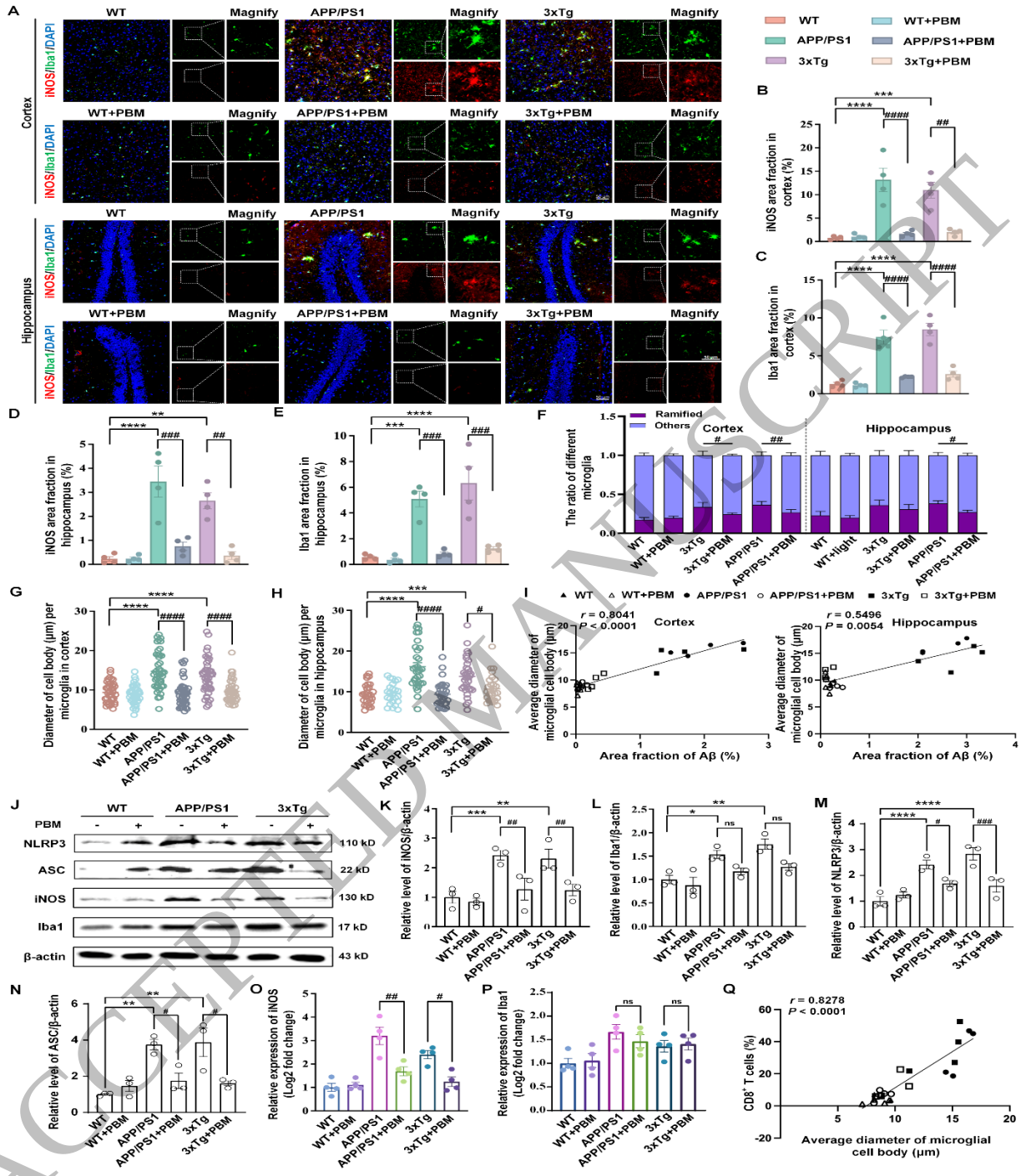

Figure 4
375x559 mm (x DPI)

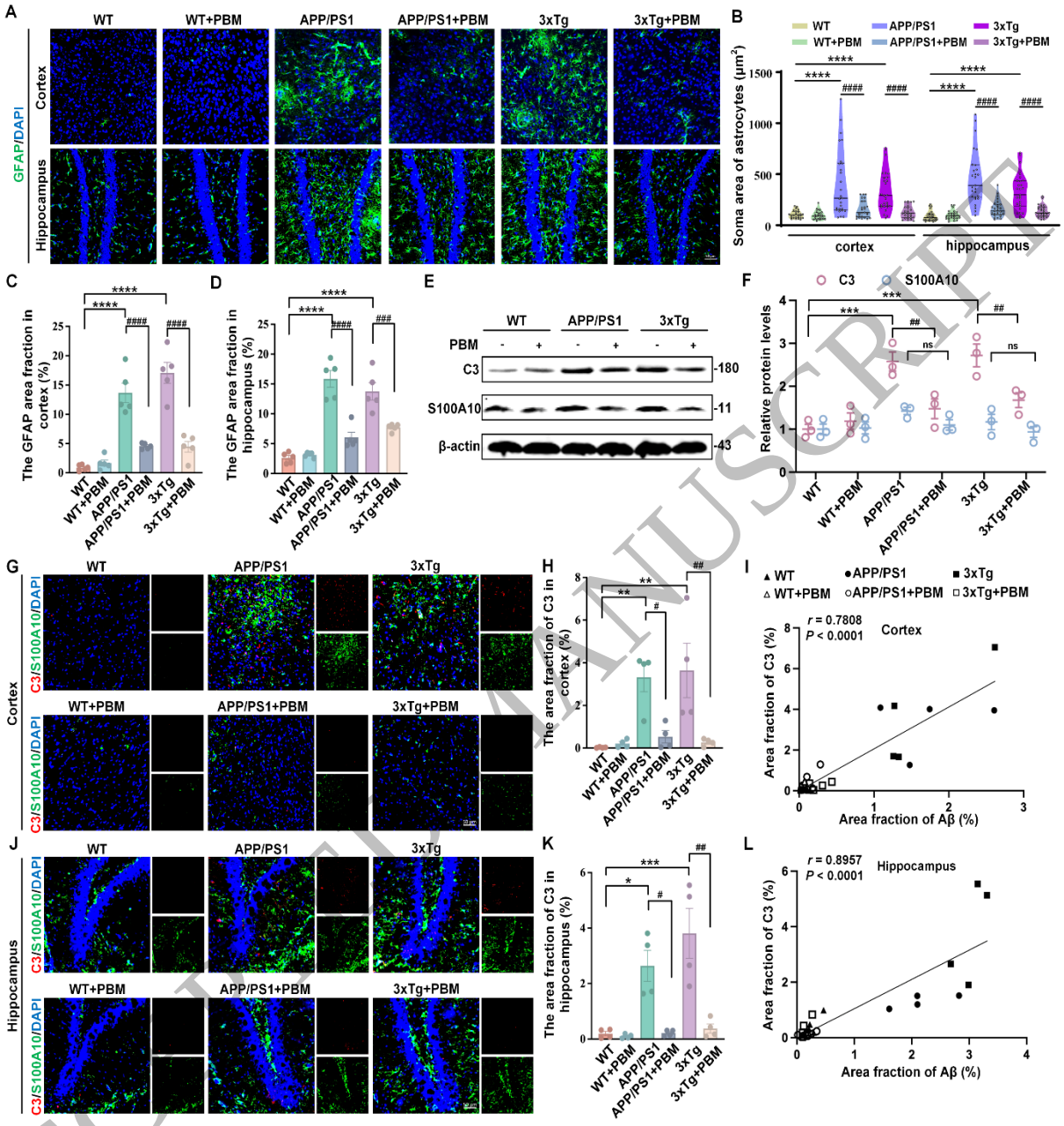

Figure 5
407x399 mm (x DPI)

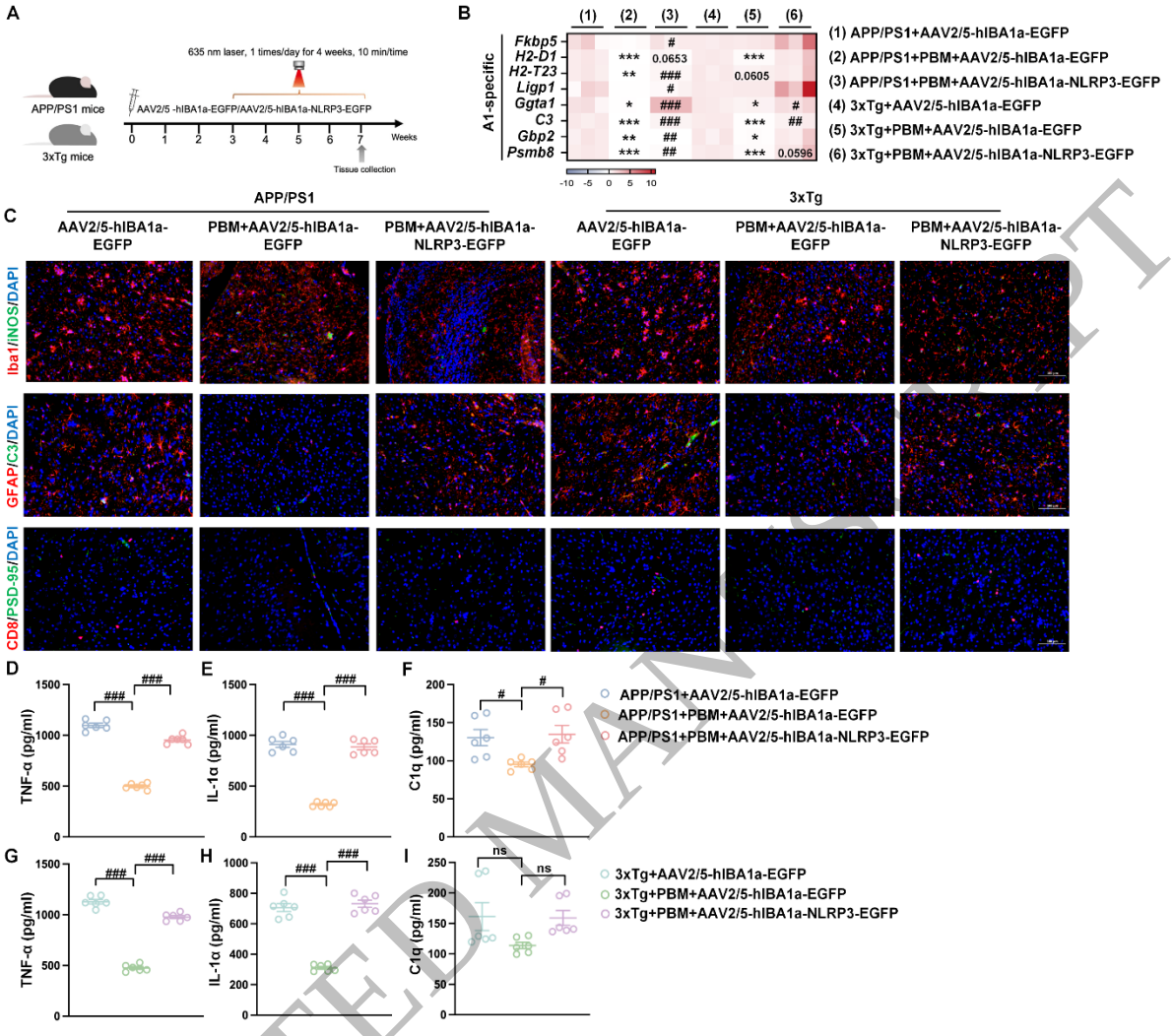

Figure 6
401x342 mm (x DPI)

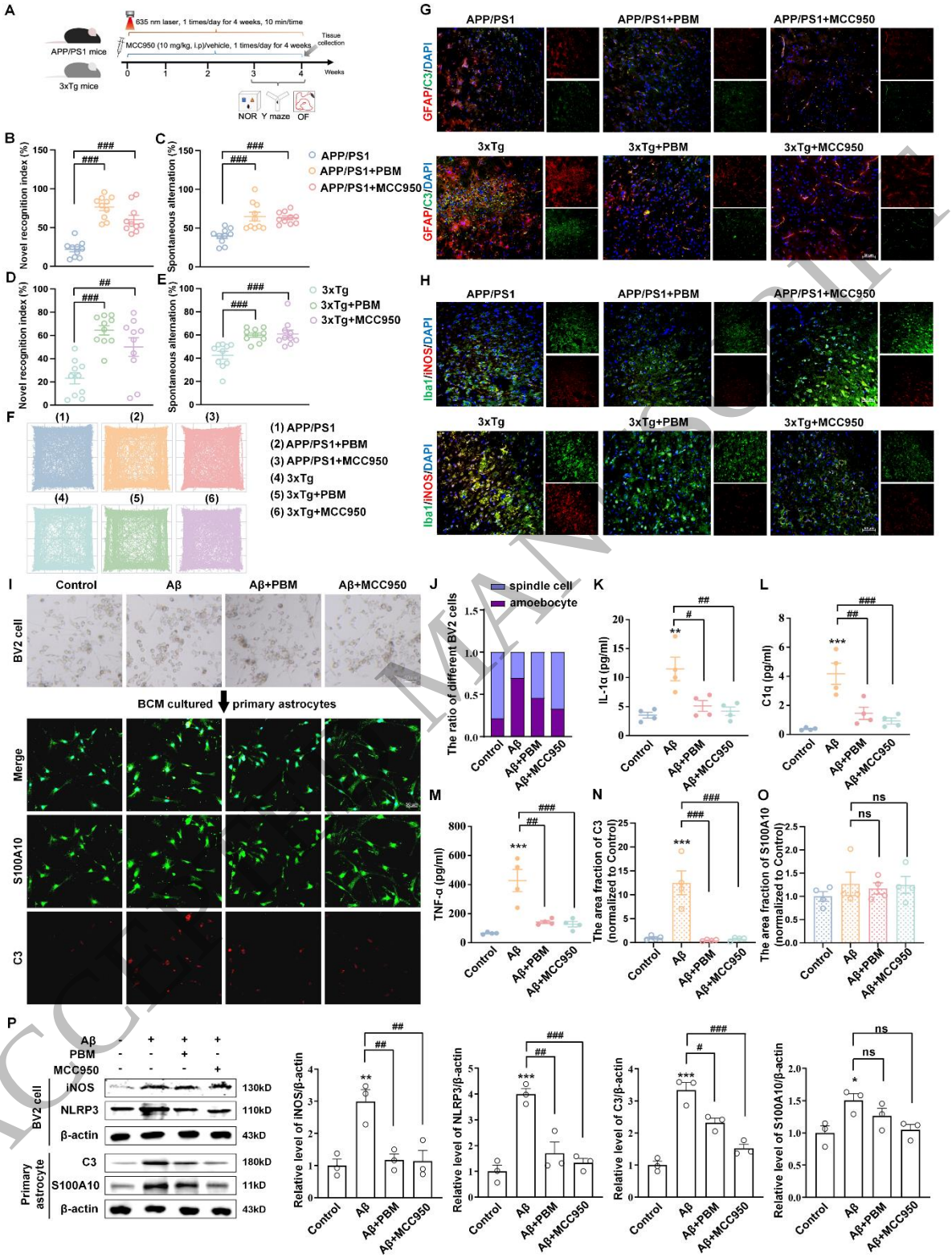

Figure 7
402x554 mm (x DPI)